

# Interactive Exemplar-based Segmentation Toolkit for Biomedical Image Analysis

Xiang Li<sup>1,2</sup>, Zhi Zhou<sup>2</sup>, Philipp Keller<sup>3</sup>, Hongkui Zeng<sup>2</sup>, Tianming Liu<sup>1</sup>, Hanchuan Peng<sup>2,\*</sup>

<sup>1</sup>Cortical Architecture Imaging and Discovery lab, Dept. Computer Science and Bioimaging Research Center, University of Georgia, Athens, GA. <sup>2</sup>Allen Institute for Brain Science. <sup>3</sup>Janelia Farm Research Campus, HHMI. \*: corresponding author

## ABSTRACT

In the field of biomedical imaging analysis on single-cell level, reliable and fast segmentation of the cell nuclei from the background on three-dimensional images is highly needed for the further analysis. In this work we propose an interactive cell segmentation toolkit that first establishes a set of exemplar regions from user input through an easy and intuitive interface in both 2D and 3D in real-time, then extracts the shape and intensity features from those exemplars. Based on a local contrast-constrained region growing scheme, each connected component in the whole image would be filtered by the features from exemplars, forming an “exemplar-matching” group which passed the filtering and would be part of the final segmentation result, and a “non-exemplar-matching” group in which components would be further segmented by the gradient vector field based algorithm. The results of the filtering process are visualized back to the user in near real-time, thus enhancing the experience in exemplar selecting and parameter tuning. The toolkit is distributed as a plugin within the open source Vaa3D system (<http://vaa3d.org>).

**Index Terms**—interactive image segmentation, learning based approach

## 1. INTRODUCTION

Cell segmentation and classification has been an important task in biological/biomedical image analysis [1-3]. Although well-discussed with various algorithms developed, it is still a challenging and data-specific problem. By recognizing the importance and potential for incorporating human prior knowledge into the segmentation process, interactive machine-learning based algorithms have been proposed in a series of recent studies, including computer vision [4] as well as on biomedical image process [5, 6]. In order to achieve an effective interactive image segmentation, there are four major challenges for the algorithm and application: 1) intuitive and easy-to-use user interface; 2) translation from implicit human domain knowledge into learning features, even for the user without image processing expertise [6]; 3) propagation of the learned features onto the whole image (i.e. classification) in an accurate, and more importantly, fast manner, thus be able to provide the near real-time feedback to the user with minimal error; and 4)

further user interaction on the results to refine the learned features and classification process.

In responding to these challenges, in this work we have proposed an interactive exemplar-based cell segmentation toolkit building on the Vaa3D system [7]. It would be shown in later sections that albeit algorithmically simple, the proposed toolkit is powerful and fast for analyzing our current dataset, where target cells are relatively homogenous but the image is large and dense. The results comparison show that our proposed toolkit outperforms widely-used segmentation techniques in both speed and accuracy.

## Related works in bioimage informatics

Among tools developed for the image segmentation in the field of bioimage informatics [8], several recent works are specifically related to our proposed toolkit. BIOCAT [2] performs both supervised and unsupervised classification using multiple classifiers based on textural, morphological, and structural features of the image. Unlike our proposed toolkit which uses interactive exemplar definition, it employs prior knowledge as a chain of selections for the features and classifiers, plus the corresponding parameters. *ilastik* [6] utilizes a similar interactive approach with our toolkit to define “labels” where several image features would be learned from their neighborhoods. Then it uses random forest classifier for the cell classification based on the learned features. The random forest classifier utilized by *ilastik* is designed for robustly handling multiple types of biological images, yet it is much slower than the filtering scheme used by our approach. On very large images, *ilastik* could hardly achieve near real-time feedback to the user, which has been shown to be an important feature of our proposed toolkit. The algorithm combining automatic clustering with supervised deconvolution proposed in [1] is also built on Vaa3D and uses 3D pinpointing interaction to define the centers of training set, while they utilized cylinder mean shift clustering to define regions around the center.

## 2. METHODS

### 2.1. Algorithm overview of the proposed toolkit

As shown in the algorithmic pipeline in Fig. 1, the proposed toolkit would first obtain the connected components of the input thresholded image through local contrast-constrained region growing (described in 2.2). Then it applies a filtering

process on the connected components to identify the “exemplar-matching” regions which are similar to the exemplar in both intensity and shape (2.3). The rest of the connected components, named “non-exemplar-matching” regions, would then be further segmented by the gradient vector field (GVF) method (2.4). The filters, as well as parameters for regions growing process, are learned from the user-specified exemplar regions (2.2).

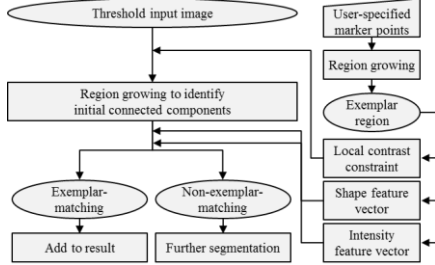


Figure 1. Pipeline of exemplar analysis and component filtering.

## 2.2. Interactive exemplar specification via Vaa3D

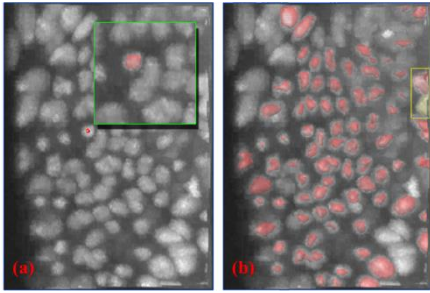


Figure 2. (a) Red dot: marker point definition by a single click from the user, its corresponding region is shown as red transparent surface in the highlighted zoomed-in view; (b) Exemplar-matching regions shown in red transparent surfaces covering the segmented cells. One non-exemplar-matching region is highlighted by the yellow box. The example further segmentation results by GVF are shown as surfaces covering this region with different colors.

The Vaa3D system that the proposed toolkit is built on provides an efficient and ergonomic platform for 3D image visualization and human interaction [7], where the user can easily rotate, zoom, pan and then perform direct 3D pinpointing on the large-scale image. As shown in Fig. 2(a), the user would only need to specify one or more marker points targeting at the desired cells in the 3D view, each with one single computer mouse operation (called “Virtual Fingers”) [9], then the exemplar region(s) would be automatically estimated and visualized from region growing results from the marker points (zoomed-in to the green box in Fig. 2(a)), providing an instant feedback. The user can also specify the marker points on the 2D tri-view window.

From the definition of exemplar regions, the toolkit extracts a set of shape feature vectors and the histogram (i.e. intensity feature vector). Specifically, to calculate the shape feature vectors for any given region, the algorithm would first obtain a bounding sphere with radius  $r$  covering the whole region with the center at the region’s center of mass.

Then three other smaller spheres with the same center but with radius of 2 (minimal),  $1/3*r$  and  $2/3*r$  are obtained, to a total of four spheres. The shape feature vector is then defined by the normalized eigenvalues of the three principle components ( $\lambda_1$ ,  $\lambda_2$ , and  $\lambda_3$ ) calculated from those four spheres:

$$S_{i,m,k} \quad m \in [1,2,3] \quad k \in [1,2,3,4] = [\lambda_1, \lambda_2, \lambda_3] / (\lambda_1 + \lambda_2 + \lambda_3) \quad (1)$$

Thus the shape feature vector could characterize the change of anisotropy from center to the boundary of the region. The proposed step-wise, anisotropy-based shape characterization is invariant to geometry transformations and scalable to region sizes, thus enabling the toolkit to generalize the pre-knowledge from the simple user input.

In addition, the average local contrast of the voxels on the exemplar region boundary versus the voxels outside the region is estimated from the unthresholded image, as the regions boundaries identification in this work are not only based on foreground/background information (i.e. growing is stopped when adjacent voxel is lower than threshold), but also constrained by the local contrast between adjacent voxels (i.e. growing is stopped when the change of intensity between adjacent voxels is too large than threshold).

## 2.3. Connected components filtering by feature-based exemplar matching

After the whole-image region growing using local maxima as seed points, the obtained connected components would then be matched with the exemplar regions based on their intensity and shape features vectors extracted in a similar fashion as for the exemplar regions. For the  $i$ -th connected component  $C_i$  with histogram  $H_i$  and shape feature vector  $S_i$ , the cost function for matching it to the  $j$ -th exemplar  $\hat{C}_j$  with histogram  $\hat{H}_j$  and shape feature vector  $\hat{S}_j$  is:

$$E(C_i, \hat{C}_j) = \left(1 - \text{corr}(H_i, \hat{H}_j)\right) + \lambda \frac{\sum_{m=1}^3 \sum_{n=1}^4 \frac{|S_{i,m,k} - \hat{S}_{j,m,k}|}{|\hat{S}_{j,m,k}|}}{\quad} \quad (2)$$

The cost function is estimated individually for each exemplar, by aggregating the costs across  $N$  exemplars and comparing to the pre-defined threshold value  $T$ , we have:

$$C_i \in \begin{cases} \text{argmin}_{\hat{C}_j \in [1 \dots N]} (E(C_i, \hat{C}_j)) \\ \emptyset, \text{ if } \min_{\hat{C}_j \in [1 \dots N]} (E(C_i, \hat{C}_j)) > T \end{cases} \quad (3)$$

Thus there would be two parameters for tuning:  $\lambda$  which balance the trade-off between intensity and shape matching, and  $T$  which balances the proportion between matching and non-matching. As the visual feedbacks of the exemplar-matching regions could be provided by our proposed toolkit in a near real-time speed, the tuning could be done interactively. An example illustration of the exemplar-matching regions is visualized in Fig. 2(b).

## 2.4. Local segmentation by GVF

GVF based image segmentation has been applied on 3D biological and biomedical image analysis with reliable accuracy [10] and has the capability of handling regions that

are closely juxtaposed or touching each other [11]. We employ the GVF method to segment the non-exemplar-matching regions that are denied by the filtering process. The algorithmic pipeline of the further segmentation route is shown in Fig. 3, and the details of the GVF method could be referred to [11]. One distinguish feature of our framework is that the GVF segmentation is performed locally on each small patches from the original image defined by the bounding box of the non-exemplar-matching regions. The rationale for the proposed toolkit to use the local GVF segmentation, rather than the global GVF which directly applied on the whole image is that: 1) the segmentation speed would be greatly increased because of the reduced input size; 2) the strategy could effectively avoid the over segmentation for connected components passed the filtering, which are the majority of regions in our working images. After local GVF, its results are then merged with the exemplar-matching regions to form the final segmentation results, which could be visualized as color-coded volumes, center markers, or contour lines as cell boundaries. The results could be easily further refined by simply adding or deleting marker points on the image then re-generate the region growing results based on the new centers.

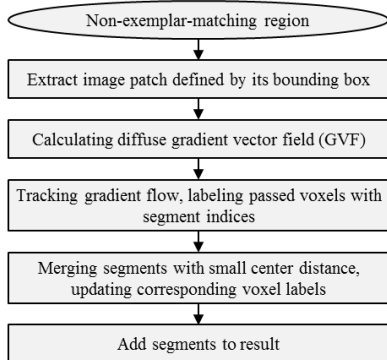


Figure 3. Algorithmic Pipeline for GVF-based segmentation.

### 3. EXPERIMENTAL RESULTS

#### 3.1. Cell segmentation on light-sheet microscopy image

In this paper, we first used the light-sheet microscopy image dataset acquired from developing drosophila melanogaster embryos [10], with dimensions 234\*222\*122, as a testing example to showcase the cell segmentation performance of the toolkit. The results of applying the toolkit on two sample images which were acquired from the same region at two different time points are shown in Fig. 4. Note that for both images, we only specified one exemplar for the feature learning, while it turned out that around 3/4 of the total connected components passed the filtering, showing that the simple feature-based filtering is an effective approach for the cell segmentation. Further, as shown by the touching cells in the zoomed-in view in Fig. 4, the filtering process recognized them as non-exemplar regions and left them for the local GVF segmentation, which correctly identified the boundaries between the touching cells.

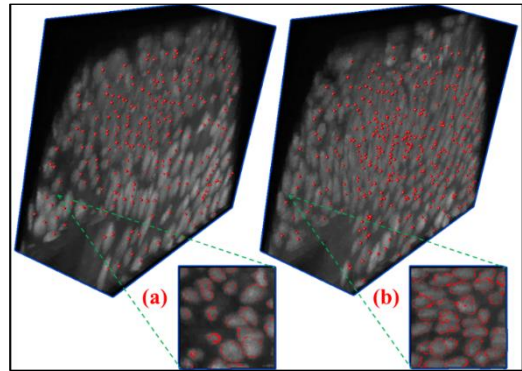


Figure 4. Cell segmentation results on two sample images. (a): results on image acquired at time point  $T_1$ , centers of the segmentation results are visualized as red dots. The zoomed-in view of the corner region shows contour lines as cell boundaries. (b): similar to (a), while the image was acquired at time point  $T_2$ .

#### 3.2 Performance comparison of the proposed toolkit

In this work, we have compared the performance (accuracy and speed) of the proposed toolkit with two widely-used unsupervised methods (watershed and GVF with adaptive threshold) and one supervised method (ilastik). The ground truth was provided by manually segmenting a portion of the sample images shown in the zoomed-in view in Fig. 4(a). Results are summarized in table 1, where Type I error indicates the percentage of the number of mis-segmented cells over the total number of cells, and Type II error indicates the percentage of the number of over-segmented cells.

	Type I Error	Type II Error	Speed
Our toolkit	5%	2%	4.1
GVF	2%	9%	10.2
Watershed	2%	>20%	43.8
ilastik	7%	>30%	25.4

Table 1. Performance comparison between methods. Speed was measured in seconds, time for interactions were excluded.

It can be seen that our proposed toolkit has similar or better performance with the other three methods, while achieving a two to ten-fold speed increase. A zoomed-in view of the comparison is visualized in Fig. 5.

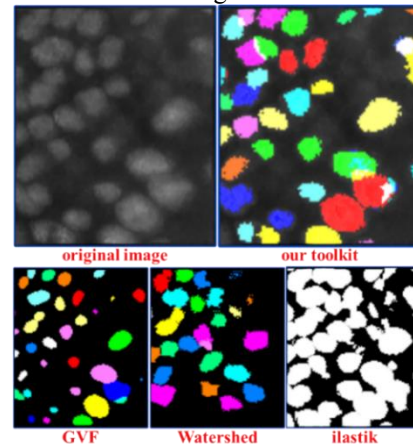


Figure 5. Comparison between cell segmentation result on a portion of the sample image between methods. Note that the output of ilastik is not color-coded by the segmentation indices, thus there is no boundary information in this visualization.

### 3.2 Neuron segmentation on mouse brain image

For further validation, we have tested the proposed toolkit on the fluorescence-labeled neuron image from mouse brain. One major challenge of the testing image is that it contains a large area with very high voxel intensity (as shown in the bright blob to the upper right and in the zoomed-in view of Fig. 6), while at the same time contains spreading cell regions with lower intensity. The experimental results shown that global GVF and watershed segmentation method could not segment these two types of regions simultaneously, even with adaptive thresholding. However, our proposed toolkit could identify most of the cells in the image even within the bright blob area, where GVF failed to detect the cells inside the blob using the same threshold value as shown in the zoomed-in view. The key reason for the improved performance of our proposed toolkit is that the local contrast constraint for the region growing process which were learned from the exemplars helps it to identify the correct boundary more robustly, thus we can use a lowered threshold for the whole image while still be able to recover the cells within high intensity background. It should be noticed that most of the segmented regions are exemplar-matching (shown as red dots) due to the relatively high homogeneity of the cell shapes in this image, which is the preferred scenario for our proposed toolkit as it lower the computational load from the further GVF routine. It took around 6 seconds for the toolkit to segment this  $1500 \times 1376 \times 10$  image (excluding human interaction time), which is much faster than global GVF and watershed. Also, it could be observed in the zoomed-in view that certain non-exemplar-matching regions segmented by our proposed toolkit are not actual cells (pointed by the yellow arrow), such region could be removed by an option in the toolkit to further filter the local GVF segmentation results.

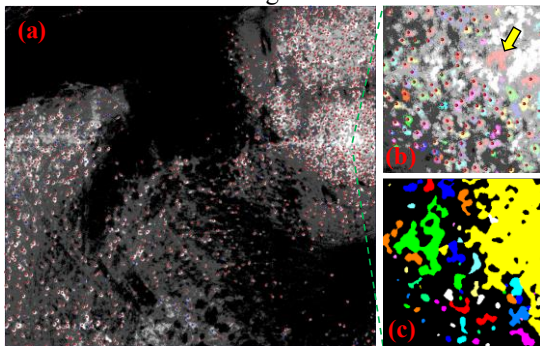


Figure 6. (a): Neuron segmentation results on sample image from mouse brain. Centers of exemplar-matching regions are visualized as red dots, centers of the GVF results are visualized as blue dots. (b): Zoomed-in view of our result, segmented regions are colored separately, only centers of the exemplar-matching regions are

shown. (c): Zoomed-in view of the segmentation result by global GVF on the whole image.

## 4. CONCLUSION

In this work we have proposed an easy-to-use interactive cell segmentation toolkit based on region features learned from user-specified exemplars, where visual feedbacks of user interaction could be provided in near real-time. Experiment results show that the proposed toolkit is both accurate and fast on the example datasets. The toolkit is open source and distributed as a plugin within the open source Vaa3D system. (<http://vaa3d.org>)

## 5. REFERENCES

- [1] Frasconi, P., Silvestri, L., Soda, P., Cortini, R., Pavone, F.S., and Iannello, G., "Large-scale automated identification of mouse brain cells in confocal light sheet microscopy images", *Bioinformatics*, 30, (17), pp. i587-i593, 2014.
- [2] Zhou, J., Lamichhane, S., Sterne, G., Ye, B., and Peng, H., "BIOCAT: a pattern recognition platform for customizable biological image classification and annotation", *BMC Bioinformatics*, 14, (1), pp. 1-14, 2013.
- [3] Kamentsky, L., Jones, T.R., Fraser, A., Bray, M.-A., Logan, D.J., Madden, K.L., Ljosa, V., Rueden, C., Eliceiri, K.W., and Carpenter, A.E., "Improved structure, function and compatibility for CellProfiler: modular high-throughput image analysis software", *Bioinformatics*, 27,(8), pp.1179-1180, 2011.
- [4] Price, B.L., Morse, B., Cohen, S., "Geodesic graph cut for interactive image segmentation", 2010 IEEE Conference on Computer Vision and Pattern Recognition, pp.3161-3168, 2010.
- [5] Veeraraghavan, H., Miller, J.V., "Active learning guided interactions for consistent image segmentation with reduced user interactions", 2011 IEEE International Symposium on Biomedical Imaging, pp. 1645-1648, 2011.
- [6] Sommer, C., Strahle, C., Kothe, U., and Hamprecht, F.A., "Ilastik: Interactive learning and segmentation toolkit", 2011 IEEE International Symposium on Biomedical Imaging: From Nano to Macro, pp. 230-233, 2011.
- [7] Peng, H., Ruan, Z., Long, F., Simpson, J., and Myers, E., "V3D enables real-time 3D visualization and quantitative analysis of large-scale biological image data sets", *Nat Biotechnol*, 28, (4), pp. 348 - 353, 2010.
- [8] Peng, H., "Bioimage informatics: a new area of engineering biology", *Bioinf (Oxford, England)*, 24(17), pp.1827-1836, 2008.
- [9] Peng, H., Tang, J., Xiao, H., Bria, A., Zhou, J., Butler, V., Zhou, Z., Gonzalez-Bellido, P.T., Oh, S.W., Chen, J., Mitra, A., Tsien, R.W., Zeng, H., Ascoli, G.A., Iannello, G., Hawrylycz, M., Myers, E., and Long, F., "Virtual finger boosts three-dimensional imaging and microsurgery as well as terabyte volume image visualization and analysis", *Nat Commun*, 5, 2014.
- [10] Tomer, R., Khairy, K., Amat, F., and Keller, P.J., "Quantitative high-speed imaging of entire developing embryos with simultaneous multiview light-sheet microscopy", *Nat Meth*, 9, (7), pp. 755-763, 2012.
- [11] Li, G., Liu, T., Tarokh, A., Nie, J., Guo, L., Mara, A., Holley, S., and Wong, S., "3D cell nuclei segmentation based on gradient flow tracking", *BMC Cell Biology*, 8(1), pp. 40, 2007.